ELSEVIER

Journal of Power Sources 92 (2001) 139–148

JOURNAL OF POWER SOURCES

www.elsevier.com/locate/jpowsour

# Gelled composite electrolyte comprising thermoplastic polyurethane and poly(ethylene oxide) for lithium batteries

Ten-Chin Wen*, Wei-Chih Chen

*Department of Chemical Engineering, National Cheng Kung University, Tainan, 701 Taiwan, ROC*

Received 15 December 1999; received in revised form 27 March 2000; accepted 24 May 2000

**Abstract**

Composite polymer electrolyte films consisting of poly(ethylene glycol) based thermoplastic polyurethane blended with poly(ethylene oxide) (denoted as TPU(PEG)/PEO) incorporating $LiClO_4$–PC have been prepared and their electrochemical properties were studied. The thermal analysis of the composite films were performed to demonstrate the miscibility of the polymer blend by using differential scanning calorimeter (DSC). TPU(PEG)/PEO based polymer electrolyte shows ionic conductivity of the order $6.4\times10^{-4}$ S/cm at room temperature, irrespective of time evolution. Cyclic voltammogram shows that this composite electrolyte has good electrochemical stability in the working voltage ranging from 2 to 4.5 V. Cycling performances of Li/polymer electrolyte/$LiCoO_2$ cells are also followed. From AC impedance results, the recharging ability of the cells is proved to be dominated by the passive layer formation at Li electrode–polymer electrolyte interface. 

*Keywords:* Lithium battery; Polymer electrolyte; Polyurethane; PEO; Polymer blending

## 1. Introduction

Ever since the reports came from Wright [1,2], poly(-ethylene oxide) (PEO) electrolytes, solid polymer electrolytes (SPE) have attracted many studies on lithium ion polymer batteries. Polymer-based solid electrolytes are of growing importance in solid-state electrochemistry in view of their applications, the most important of which is in high-energy-density batteries. Most of the researchers have concentrated on designing novel polymer materials possessing high ionic conductivity, good mechanical properties as well as thermal stability for technological applications [3–8].

The polymer electrolyte based batteries are actively being developed because of their advantages in comparison to conventional systems containing liquid electrolytes. For instance, polymer electrolyte batteries can be manufactured inexpensively from structural units composed of anode, cathode and electrolyte laminates. Moreover, the solid-state modular batteries allow fabrication in a varied range of sizes and shapes. Another attractive feature of polymer electrolyte batteries is that they can be designed in bipolar configuration for multicell batteries without the intercell leakage current and the associated self-discharge problems encountered in liquid electrolyte systems [9]. The polymer electrolyte lithium batteries contain all solid-state components: lithium as the anode material (alternatively, carbon is used as anode to improve cycling safety), a thin polymer film as the solid electrolyte, a separator, and a transition metal chalcogenide or oxide as the cathode material [10]. Applications such as mobile telephones, smart credit cards, and notebook computers require thin flat batteries which can readily be fabricated from polymer electrolyte systems.

Among the interesting polymer electrolytes that were developed, polyether-based electrolytes showed features such as good adherence to electrodes and the ability to solvate many inorganic salts. Ionic conductive polymers such as complexes of PEO and lithium salts, which showed high ionic conductivity of $10^{-4}$ to $10^{-3}$ S/cm at high temperatures were characterized by a bi-ion transport mechanism [11–14]. In the PEO–LiX ($X=ClO_4^-$, $CF_3SO_3^-$) system, the PEO provides the ethylene oxide structure to stabilize the lithium ion and to uncoil the polymer chain for migration of ions. However, the PEO–LiX system shows poor conductivity at room temperature because the ions possess low mobility in PEO film due to its high crystallinity.

Although there is no common agreement on the exact mechanism of ionic transport in polymer-based electrolytes, it is conceivable that significant motion exists only in the

* Corresponding author. Tel.: +886-6-2385487; fax: +886-6-2344496.
*E-mail address*: tcwen@mail.ncku.edu.tw (T.-C. Wen).

0378-7753/01/$ – see front matter 
PII: S0378-7753(00)00510-3

amorphous phase of polymers while nonconducting in the crystalline phase [15]. Thus, in order to design an excellent polymer electrolyte, the degree of crystallinity of the polymer should be lowered, while adequate mechanical properties should be maintained for practical applications. Ease of film fabrication is another necessary and important factor consideration. However, pure PEO is a semicrystalline polymer, possessing both amorphous and crystalline phases at room temperature. Hence, considerable ionic conductivity in PEO-based polymers can only be obtained at high temperature [16]. From the above fundamental knowledge, designing of novel polymer with similar characteristics of PEO is needed. It is reasonable that a PEG reacted with diisocyanate to form a PEG-based thermoplastic polyurethane (TPU(PEG)). This TPU belongs to an elastomer class possessing high tensile strength, elasticity as well as low crystallinity. Our laboratory has reported several papers about PU-based polymer electrolytes [17–24].

While forming polymer matrix suitable for polymer electrolyte formation, the polymer is usually mixed with a small polar solvent (plasticizer) such as ethylene carbonate (EC) or propylene carbonate (PC), which is used to improve conductivity [25]. This category of polymer electrolyte containing polar solvent is called gel-type electrolyte. In this case, the solvent plays the role of the ion supporting carrier and the plasticizer of polymer matrix, enhancing the mobility of ions and flexibility of polymer electrolyte. Unfortunately, the addition of solvents always weakens the polymer strength and also causes insulation between anode and cathode.

For polymer electrolytes to be of practical use, Li-ion mobility must be high enough to enable useful rate capabilities in Li batteries. For safety, storage, and cycle life the electrolyte must be chemically stable with the electrode contact. In high voltage cells, the electrolyte must also be electrochemically stable over the potential window of the electrode couple. The objective of the present work is to study the electrochemical properties of composite electrolytes involving TPU and PEO.

## 2. Experimental

### 2.1. Synthesis of thermoplastic polyurethane (TPU)

Poly(ethylene glycol) (PEG, $\overline{M}_w$=1000, Showa Chemical Inc.) was dried and degassed in a vacuum oven under 85°C for 1 day. All other chemicals were used without further treatment.

An outline of the process used in this study for preparation of PEG based TPU dispersions (noted as TPU(PEG)) is shown in Scheme 1. The TPU(PEG) prepolymer was synthesized by a one-step addition reaction. The reactor was a 2000 ml four-necked round-bottom flask equipped with an anchor-propeller stirrer, a nitrogen inlet and outlet and a thermocouple connected to the temperature controller.

PEG (100 g, 0.1 mol) and methylene-bis-(*p*-cyclohexyl isocyanate) ($H_{12}$MDI, Aldrich) (81.33 g, 0.31 mol) were simultaneously added to the reactor which was charged under a nitrogen gas atmosphere, to form a prepolymer of TPU where the ratio of NCO/OH is 3. The temperature was kept at 50°C initially. After proper mixing (100 rpm), two drops of di-*n*-butyltin(IV) dilaurate (DBTDL, catalyst) were added into the batch to catalyze the reaction and then the temperature was raised at 85°C. After 6 h of reaction, 700 g of dimethylformamide (DMF, Tedia Company Inc.) was added. And then the chain extender, ethylenediamine (EDA, Merck) (12.6 g, 0.21 mol) which was previously diluted to a 10% solution in DMF, was added slowly to convert the prepolymer into polymer. The viscosity was found to increase in this step. After 1 h reaction, several drops of methyl alcohol (MeOH, Tedia Company Inc.) were added to terminate the reaction.

### 2.2. Molecular weight

The average molecular weights, $\overline{M}_n$ and $\overline{M}_w$, were determined by use of a Shimadzu GPC fitted with a Shimadzu HPLC pump and a differential refractometer. A Jordi gel DVB mixed-bed 250 mm×10 mm column was employed for the analysis. DMF was used as the continuous phase and was pumped through the column at a flow rate of 2.0 ml/min. This system was calibrated against 10 polystyrene standards. The measured molecular weight and molecular weight distribution of the synthesized TPU(PEG) are given here, $\overline{M}_n=8.9\times10^4$, $\overline{M}_w=24.9\times10^4$ and the polydispersity index is 2.79.

### 2.3. Preparation of the composite electrolytes

The prepared TPU(PEG) blend was mixed with the DMF solution of poly(ethylene oxide) (PEO, $\overline{M}_w=4\times10^5$, Aldrich) in 1:1 weight ratio to form uniform solution. This solution was then heated and stirred under 70°C for 4 h and coated on a glass dish to be a film. The film was then dried under vacuum at 50°C for 7 days and stored in an argon filled dry box (M. Braun Company, Germany). The thickness of the film was controlled to be about 190 μm.

Lithium perchlorate, $LiClO_4$ (anhydrous, Anderson Phys. Lab.) was dissolved in propylene carbonate (PC, anhydrous, 99.7%, Aldrich) to form 1 M $LiClO_4$–PC solutions in dry box.

The composite electrolyte was prepared by dipping dried TPU(PEG)/PEO composite film into 1 M $LiClO_4$–PC solution for 10 min at room temperature in a dry box. The percentage increase in weight due to swelling with respect to swollen weight, $S_w$, was determined by using

$$S_w = \frac{100(W - W_0)}{W}$$

$W_0$ is the weight of the dried film and $W$ is the weight of the film at 10 min swelling.

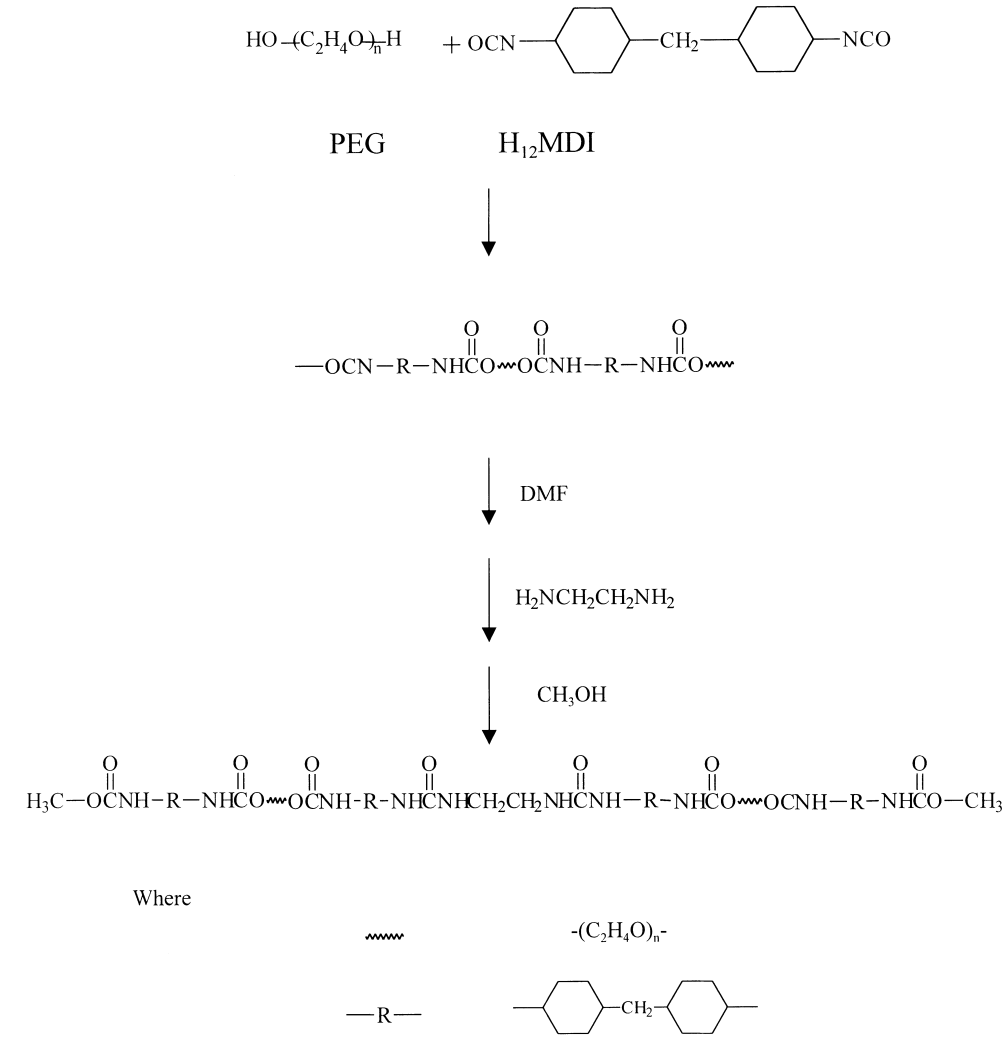


Scheme 1. Polymerization of thermoplastic polyurethane.

### 2.4. Thermal analysis

Thermal analysis of the composite films was carried out on a DuPont DSCr 2010 differential scanning calorimeter with a heating rate of 10°C/min and over the temperature range of −100 to 100°C. Samples taken from the composite films were sealed in aluminum capsules and transferred out of dry box to perform thermal analysis.

### 2.5. Conductivity measurement

The conductivity of the composite electrolyte (37.5% TPU(PEG)/PEO and 62.5% $LiClO_4$/PC) was measured via impedance analysis with an electrochemical cell consisting of the electrolyte film sandwiched between two blocks of stainless steel, sealed with an O-ring in a tube which was covered with jacket for heating/cooling water circulation. The temperature of the cell was controlled using a water thermostat (HAAKE D8 & G) and calibrated using a Pt resistance thermometer. The impedance analysis was performed by using an Autolab PGSTAT 30 equipment (Eco Chemie B.V., Netherlands) with the help of frequency response analysis system software under an oscillation potential of 10 mV from 100 kHz to 1 kHz.

### 2.6. Assembly of laminated cell

Lithium metal and $LiCoO_2$ were employed as negative and positive electrodes, respectively. The area of both electrodes was fixed to 2.25 $cm^2$. Then, Li/polymer electrolyte (PE)/$LiCoO_2$ laminated cells were assembled by pressing Li, PE, and $LiCoO_2$; sealed by polyethylene laminating film; laminated by an aluminum foil. Afterwards, the cells were cycled with BT-2043 system (Anbin electrochemical instrument, USA) between 4.2 and 2.7 V at room temperature.

### 2.7. Cyclic voltammetry measurement

Cyclic voltammetry was performed to determine the electrochemical stability window of the electrolytes using a three-electrode cell. The working electrode was stainless

steel (SS, the type is stainless steel 304) and kept the area at 1 $cm^2$, and lithium metal was utilized for both the counter and reference electrodes. Measurements were performed on Autolab PGSTAT 30 equipment with general purpose electrochemical system software at room temperature.

### 2.8. Interfacial resistance measurement

The interfacial corrosion measurements were performed with a Li/PE/Li laminated cell with nickel net current collectors at room temperature by using an Autolab PGSTAT 30 equipment with the help of frequency response analysis system software under an oscillation potential of 20 mV from 100 kHz to 0.1 Hz.

## 3. Results and discussion

### 3.1. Thermal analysis

In order to investigate the degree of miscibility of TPU-(PEG)/PEO blend, differential scanning calorimeter analysis was performed. Fig. 1 shows the glass transition ($T_g$) temperature of three polymers and in each thermogram, the $T_g$ are shown by arrows. A comparison among curves A, B and C reveals that the $T_g$ of PEO shifts to a higher temperature, and the $T_g$ of TPU(PEG) shifts to a lower temperature as TPU(PEG) and PEO were blended. These results validate that TPU(PEG)/PEO blend is partially miscible. The above results can be reasonably explained from the view point of the molecular structures of TPU(PEG) and PEO. The repeat unit of PEO is –(C–C–O)–. Since TPU(PEG) also possesses the same type of repeat unit, –(C–C–O)–, for its soft segment, it is reasonable to consider that TPU(PEG) is partially miscible with PEO.

### 3.2. Arrhenius plot of conductivity

The temperature dependency of the conductivity of the gel electrolyte film is shown in Fig. 2. The figure shows a straight line, indicating that the conductivity of polymer electrolyte obeys Arrhenius law. This implies that the conductive environment of $Li^+$ in the polymer electrolyte is liquid like and remains unchanged in the investigated temperature region. From Fig. 2, it is clear that the conductivity increases evidently with increasing temperature and the conductivity at 25°C was calculated to be $6.4\times10^{-4}$ S/cm. The activation energy ($E_c$) of conductivity for this film can be calculated from Arrhenius equation

$$\sigma = \sigma_0 \exp\left(\frac{-E_c}{RT}\right)$$

where $T$ is temperature on the Kelvin scale and $\sigma_0$ is a proportional constant. $E_c$ value of this polymer film is 19.6 kJ/mol and this value is low. For instance, in our previous paper [24], $E_c$ values of TPU(PEG), TPU(PTMG), and PEO are 29.3, 40.6, and 30.8 kJ/mol, respectively.

### 3.3. Cyclic voltammetry studies

The cyclic voltammogram (CV) for the Li/PE/SS cell at room temperature is given in Fig. 3. The sweep rate was kept as 5 mV/s. The CV indicates a stable electrochemical potential window on stainless steel of 1.5 to 4.5 V versus $Li/Li^+$ and hence it can be taken that the stability window is at least 4.5 V. The CVs pattern of typical liquid $LiClO_4$/PC electrolytes and in the presence of gel electrolytes are nearly the same. This indicates that TPU(PEG)/PEO has no effect on the stability window of the electrolyte. The onset potential for Li deposition on SS was about −0.05 V and it is can be taken as cathodic limit. Li stripping is observed by the

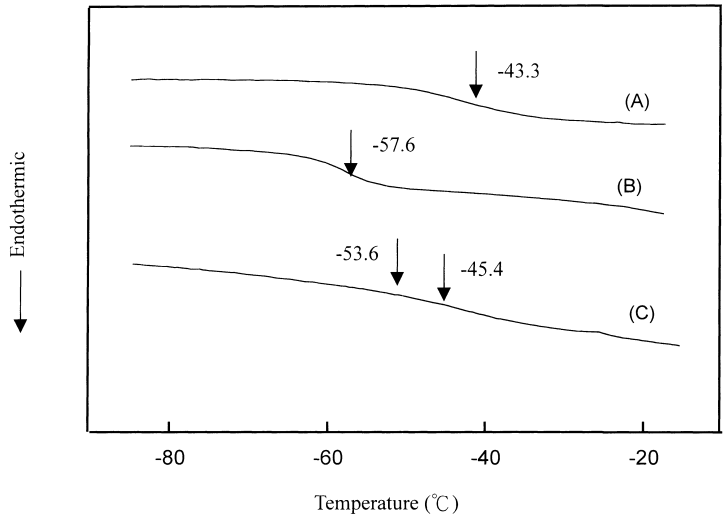


Fig. 1. DSC thermograms of: (A) TPU(PEG), (B) PEO, (C) TPU(PEG)/PEO blend.

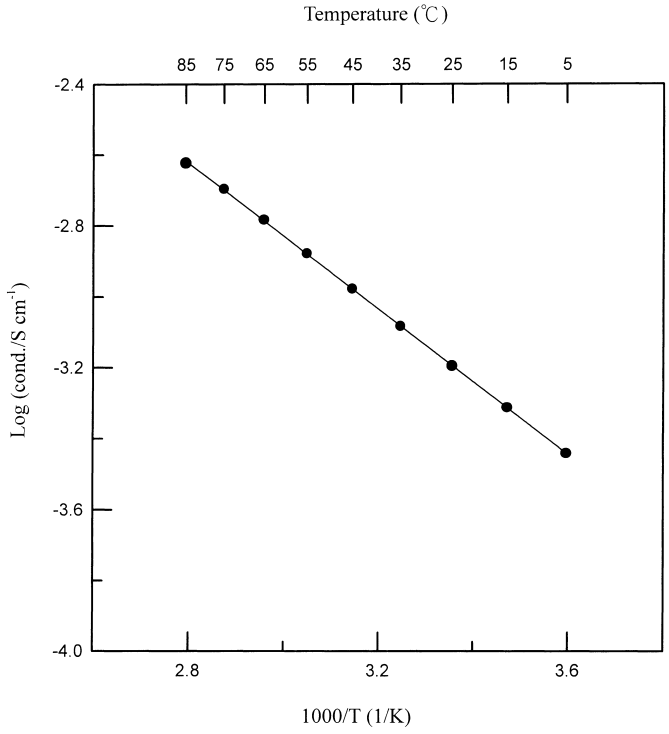


Fig. 2. Arrhenius plot of ionic conductivity for gel electrolyte containing 62.5% of 1 M $LiClO_4$–PC.

anodic peak at 0.52 V and delithiation of the alloy formed is at 0.92 V. This plating–stripping process is reversible, the kinetics are fast but the reversibility tends to decrease with cycling. As can be seen in Fig. 3, there are no more oxidation peaks up to 4.5 V (versus $Li/Li^+$). Thus, the TPU(PEG)/PEO-based polymer electrolyte in this work has displayed sufficient electrochemical stability to allow safe operation in rechargeable lithium battery systems. The reasons for this

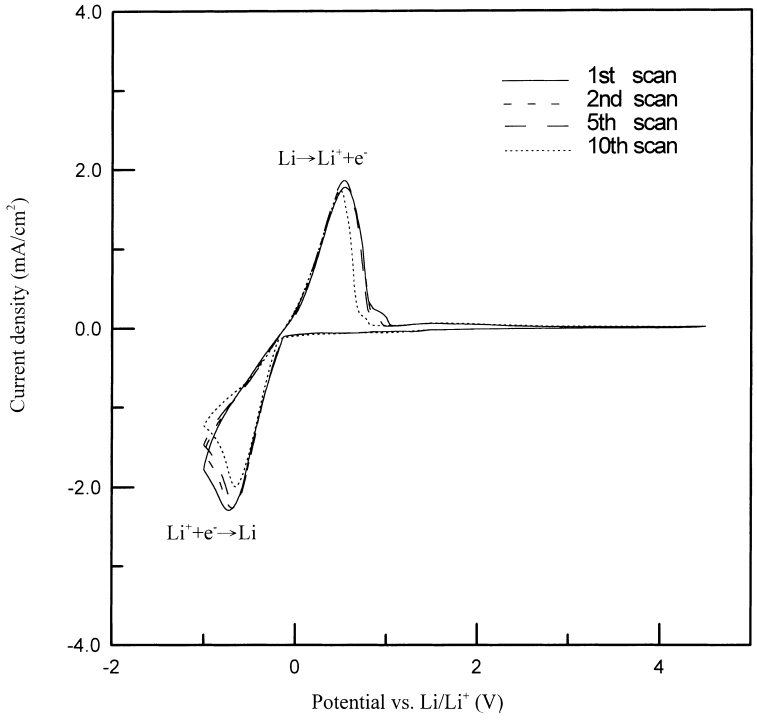


Fig. 3. Cyclic voltammogram for Li/PE/SS cell, sweep rate: 5 mV/s.

good electrochemical stability for our system can be viewed on line with other reports.

Some reports [26,27] presented that the additions (organic solvents and lithium salts) of PAN-based polymer electrolyte appear to influence the oxidation potential. Accordingly, the oxidative stability of organic esters (PC and EC) is higher than that of ethers and the PAN–$LiClO_4$-based electrolyte has higher electrochemical stability than any of the other PAN–lithium salt based electrolytes. Since the $LiClO_4$ lithium salt has a higher lattice energy than any of the other lithium salts, the interaction between the polymer and the lithium salt is relatively small, this effect influences the electrochemical stability window. Although $LiPF_6$ has the lowest thermal stability of all lithium salts and greater sensitivity to moisture, the electrochemical oxidative stability is adequate and there is less corrosion with an aluminum current-collector.

### 3.4. AC impedance studies

AC impedance spectroscopy was used to investigate the interface between Li metal and gel-electrolyte. For the assembled cell, Li/polymer electrolyte/Li, time evolution of the impedance response was monitored for several weeks and the results are presented in Fig. 4. An examination of Fig. 4 reveals that all curves are similar in shape with arcs in high frequency region and straight lines in low frequency region. At very low frequency region, the diffusion of active species determines the impedance response. This is as a result of charging of double layer during potential oscillation with an occurrence of charge transfer reaction between electrode surface and electrolyte. As a consequence, a straight line in Nyquist plot, so called 'Warburg diffusion impedance' was obtained. With increasing frequency, the charge transfer reaction during potential oscillation decreases so that the effects of the diffusion of active species on impedance response decreases. Thus, the response makes a minimum at a certain frequency (noted as $f_w$). At the frequency close to $f_w$, the impedance response aggregates together and approaches the real axis, and as a result the combined value of charge transfer resistance ($R_{ct}$) and bulk resistance ($R_b$) was obtained. At frequency larger than $f_w$, the impedance response is determined by dynamics of interfacial reactions. Thus, a semicircle response is obtained and can be simulated by RC circuit of $R_{ct}$ and $C_d$ (double layer capacitance) in parallel. At the frequency of approximating 100 kHz, the impedance response is close to the real axis again. The value obtained from this approximation is represented as $R_b$. The equivalent circuit model is shown in the insert of Fig. 4, in which Warburg diffusion impedance can be eliminated in the case of frequencies larger than $f_w$. Thus the total impedance ($Z$) can be simplified as following:

$$Z = \left(R_b + \frac{R_{ct}}{1 + (R_{ct}\omega C_d)^2}\right) - \left(\frac{R_{ct}^2 \omega C_d}{1 + (R_{ct}\omega C_d)^2}\right) j \qquad (1)$$

where $\omega$ is the angular frequency and $j$ represents the imaginary part of $Z$. The denominator term, $1+(R_{ct}\omega C_d)$ in Eq. (1), relating the order of magnitude of dimensionless group, $R_{ct}\omega C_d$, in comparison with unity, is very important for the analysis of a physical system. According to engineering viewpoint, there are two extreme cases (i) when

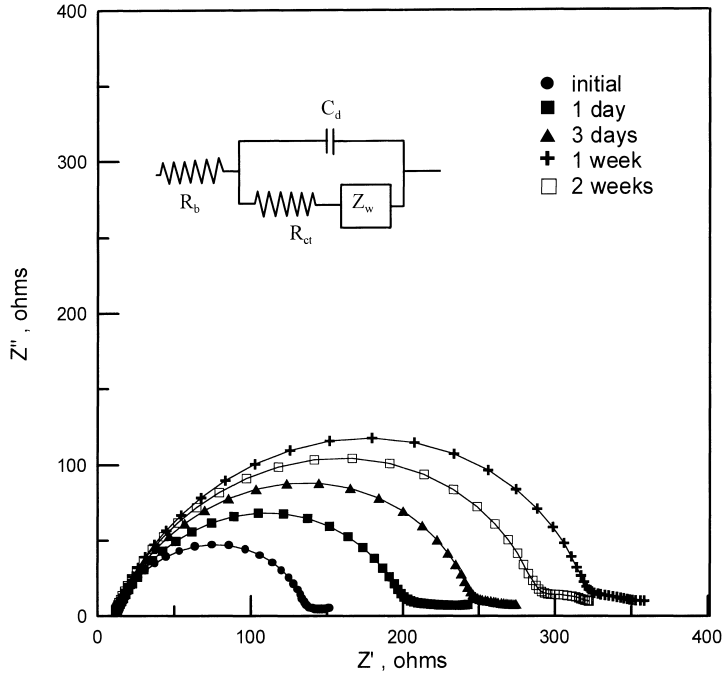


Fig. 4. Time evolution of the impedance response of Li/PE/Li cell at room temperature.

$R_{ct}\omega C_d \gg 1$, then $Z \rightarrow R_b$, while (ii) when $R_{ct}\omega C_d \ll 1$, then $Z \rightarrow R_b + R_{ct}$.

As can be seen in Fig. 4, the values of $R_b$ are almost the same in each curve. This means that the encapsulated liquid electrolyte in the polymer chains has not lost its electrochemical properties because of the non-volatile nature of the organic solvent and exhibits good compatibility with the lithium electrode. The value of $R_{ct}$ was found to increase quickly during the first week and became stabilized at a value of 280 Ω after 2 weeks. This phenomenon can be attributed to the formation of a passive layer due to the reactivity of the electrode and the electrolyte. Aprotic solvents such as PC and EC are well known to form passive layers on Li metal. Growth of these resistive layers will increasingly prevent Li-ion transport and thus block the flow of current through the cell.

$C_d$ was determined from the top point of the semicircle on Nyquist plot, as an extreme value in the imaginary part of Eq. (1). By differentiating the imaginary part and letting the result equal to zero, $C_d$ was obtained from the following equation:

$$R_{ct}\omega_m C_d = 1 \quad (2)$$

where $\omega_m$ represents the angular frequency at the top point of the semicircle on Nyquist plots. The values of $C_d$ were found to be close to 0.34 μF in all the cases. The constancy of $C_d$ may represent the possible maximum accumulating charge on the surface of polymer electrolyte and can be considered as independent of the storage time.

### 3.5. Cycling performance

In order to investigate the utility of the TPU(PEG)/PEO-based polymer electrolyte when combined with an anode and a cathode in a lithium ion polymer battery, a Li/PE/$LiCoO_2$ cell has been constructed. The theoretical capacity of the $LiCoO_2$ electrode is 120 mAh/g. Cycling tests were performed at three different cycling rates (C/10, C/7 and C/4) and with cut-off voltages as 4.2 and 2.7 V for the upper and lower limits respectively. The cut-off voltage is so selected to prevent destroying of the crystallinity of $LiCoO_2$. In the charge reaction, the $x$ in $Li_xCoO_2$ gradually decreases from $x=1$ to $x=0.55$. For values of $x$ lower than 0.55, the oxidation of $Co^{3+}$ to $Co^{4+}$ becomes possible [28,29] which may also transform the crystallinity of cathode affecting the crystal structure and thus cause decreasing in reversibility. Therefore, the depth of discharge is limited to less than 120 mAh/g of $LiCoO_2$ to keep up the cycling performance.

The charge–discharge curves of Li/PE/$LiCoO_2$ cells at the third cycle are given in Fig. 5. This figure reveals that the cell at C/10 rate can achieve a good capacity of 116.85 mAh/g. At high rates C/7 and C/4, however, the capacity is less than that at C/10 rate; it is found that the reversible capacity decreases as the current rate increases. A comparison among the discharge curves, the capacities at C/7 and C/4 rates are 82% and 62% of the capacity at C/10 rate, respectively. It is concluded that the reduced capacity at high rates is due to the low value of the chemical diffusion coefficient of lithium ions in the lattice of $LiCoO_2$ and lower diffusion rate of

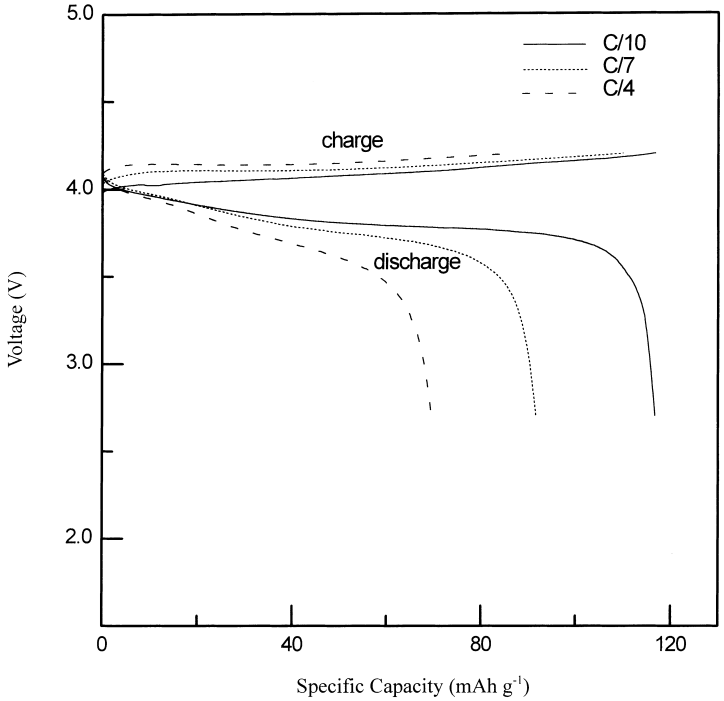


Fig. 5. The third cycle charge–discharge performance of Li/PE/$LiCoO_2$ cells at different cycling rates.

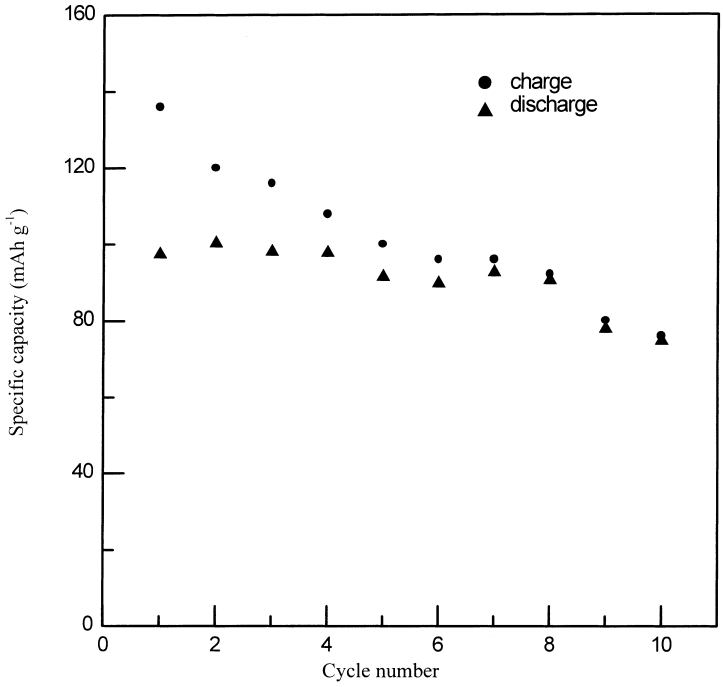


Fig. 6. Charge and discharge capacity of a Li/PE/$LiCoO_2$ cell as a function of cycle number at C/10 rate.

lithium ions in the polymer electrolyte as compared with that in liquid electrolyte.

The charge–discharge capacity and coulombic efficiency of the Li/PE/$LiCoO_2$ cell as a function of cycle number are showed in Figs. 6 and 7, respectively. The charge capacity of the cell declines as the cycle number increases, and after 10 cycles, the capacity is about two-third of the theoretical capacity. The coulombic efficiency is estimated to be more than 90% after initial three cycles and even reaches near 100% after seven cycles. The large irreversible capacity observed in the first cycle is due to the formation of a passive film on the surface of the lithium electrode, which results

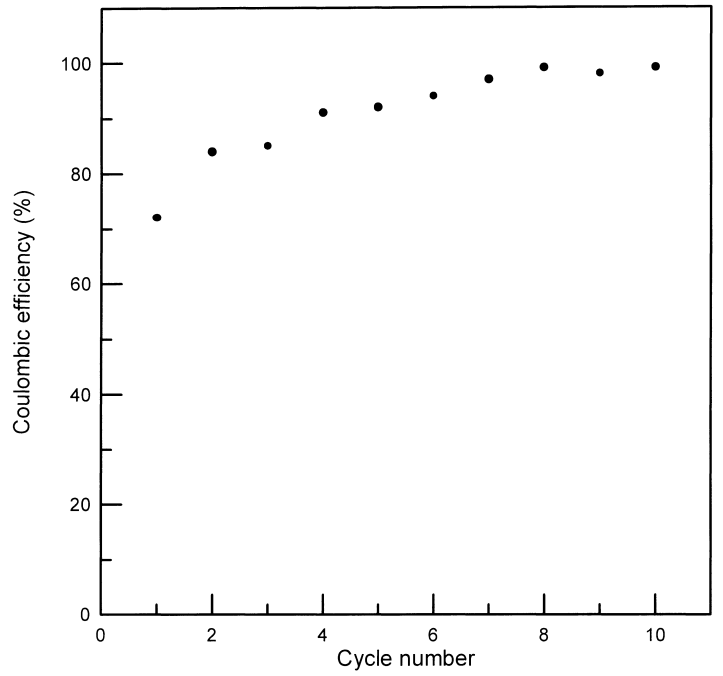


Fig. 7. Coulombic efficiency of a Li/PE/$LiCoO_2$ cell as a function of cycle number at C/10 rate.

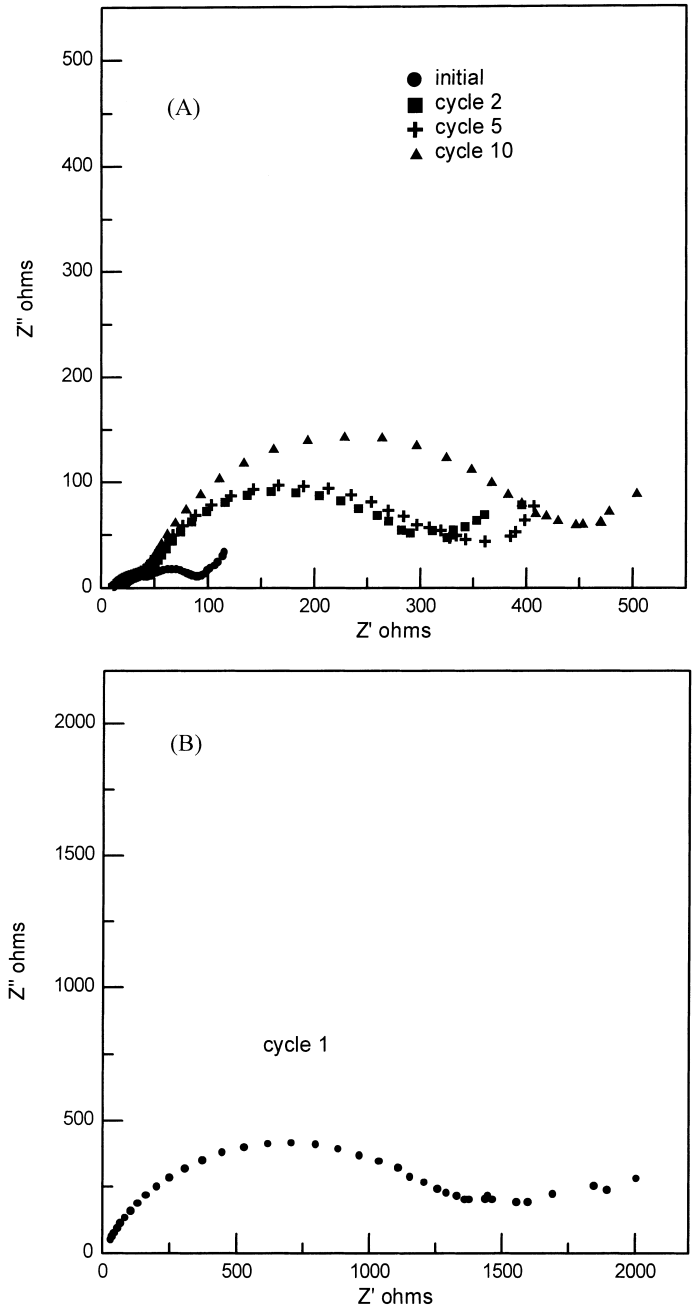


Fig. 8. AC impedance spectrum of the Li/PE/$LiCoO_2$ cell at different cycles.

from the presence of PC solvent. The above results can be reasonably explained from the AC impedance measurements in Fig. 8.

AC impedance spectra of a Li/PE/$LiCoO_2$ cell before and after several cycles are given in Fig. 8. The four curves in Fig. 8(A), all display two semicircles and a straight line. The larger semicircle, at middle frequency, can be associated with the interfacial resistance at the lithium electrode. The high-frequency semicircle is related to the impedance of a surface layer formed on the $LiCoO_2$ surface. And the straight line is Warburg diffusion impedance between electrode and electrolyte. For a freshly made cell, the two arcs are very small, but after the first charge–discharge cycle, the interfacial resistance on the Li surface increases greatly (Fig. 8(B)), and then decreases to a lower value in the later cycles. The above results can explain the reasons of low coulombic efficiency at cycle 1 and higher efficiency at later cycles. This behavior can be ascribed to an initial poor interfacial contact between the polymer electrolyte and Li electrode before charge–discharge cycling. This necessitates Li/PE interface to activate initially by using current flow. In further cycling, the middle-frequency semicircle increases

as the cycle number increases and this semicircle is deformed by Warburg diffusion impedance (Fig. 8(A)). The definition of Warburg diffusion impedance is given as

$$Z_w = \frac{\sigma}{\sqrt{\omega}}(1 - j)$$

where $Z_w$ is Warburg impedance, $\sigma$ is the Warburg impedance coefficient, $\omega$ is the angular frequency, and j represents the imaginary part of $Z$. The Warburg impedance, $Z_w$, is controlled by $\sigma$. If $\sigma$=0, means there only semicircles exist without Warburg impedance effects. As $\sigma$ value increases, the end of the middle-frequency semicircle appears as a diffusion tail. When $\sigma$ increases to equal $R_{ct}$ value, this diffusion tail overlaps with the semicircle, and the straight line at an angle of 45° to the real axis occurs. If $\sigma$ continues increasing, the overlap condition is more serious and the shape of the semicircle is deformed greatly. In Fig. 8(A), the middle-frequency semicircle in cycle 10, the $R_{ct}$ value is largest and the shape deformation is most serious. This result reveals that when the cycle number increases, the charge transfer in the lithium electrode is difficult and $Li^+$ ion diffusion rate in the Li/PE interface becomes very slow. This is a convincing indication of the reaction between PC and lithium metal to result a passive layer which would cause loss of capacity on cycling due to degradation of Li/PE interface. Therefore, it is concluded that the passive layer formed at the Li/PE interface dominates the rechargeable ability of cells.

## 4. Conclusion

The TPU(PEG)/PEO-based gel polymer electrolyte displays high conductivity at room temperature and possesses good electrochemical stability in the working voltage range to allow the operation in a Li/PE/$LiCoO_2$ rechargeable lithium battery. Due to the existence of liquid solvent PC, a passive layer is formed on the Li/PE interface. From the view point of AC impedance studies on the cycling performance of a Li/PE/$LiCoO_2$ cell, the capacity loss and low coulombic efficiency are reasonably explained by the lithium electrode–polymer electrolyte interface resistance. This makes rechargeable ability of cells to dominate by the passive layer formation at the Li/PE interface.

## Acknowledgements

The financial support of this work by the National Science Council of the Republic of China under contract NSC 89-2214-E-006-012, is gratefully acknowledged.

## References

[1] P.V. Wright, Br. Polym. J. 7 (1975) 319.
[2] M.B. Armand, Solid State Ionics 9/10 (1983) 745.
[3] C.H. Yang, S.M. Lin, T.C. Wen, Polym. Eng. Sci. 35 (1995) 722.
[4] K. Murata, Electrochim. Acta 40 (1995) 2177.
[5] D. Fauteux, A. Massucco, M. Mclin, M. van Buren, J. Shi, Electrochim. Acta 40 (1995) 2185.
[6] S. Slane, M. Salomon, J. Power Sources 55 (1995) 7.
[7] D.W. Kim, J. Power Sources 76 (1998) 175.
[8] H.S. Kim, B.W. Cho, J.T. Kim, K.S. Yun, H.S. Chun, J. Power Sources 62 (1996) 21.
[9] K.M. Abraham, Electrochim. Acta 38 (1993) 1233.
[10] D. Linden, Handbook of Batteries, McGraw-Hill, New York, 1995, p. 36.9
[11] J. Barthel, R. Buestrich, E. Carl, H.J. Gores, J. Electrochem. Soc. 141 (1996) 3565.
[12] H.S. Lee, X.Q. Yang, J. McBreen, Z.S. Xu, T.A. Skotheim, Y. Okamoto, J. Electrochem. Soc. 141 (1994) 886.
[13] T. Shodai, B.B. Owens, H. Ohtsuka, J. Yamaki, J. Electrochem. Soc. 141 (1994) 2978.
[14] K.V. Ramanujachary, X. Tong, Y. Lu, J. Kohn, M. Greenblatt, J. Appl. Polym. Sci. 63 (1997) 1449.
[15] C. Berthier, W. Gorecki, M. Minier, M.B. Armand, J.M. Chabagno, P. Rigand, Solid State Ionics 11 (1983) 91.
[16] G.C. Farrington, R.G. Linford, in: J.R. MacCallum, C.A. Vincent (Eds.), Polymer Electrolyte Reviews 2, Elsevier, London, 1989, p. 255.
[17] T.C. Wen, Y.J. Wang, T.T. Cheng, C.H. Yang, Polymer 40 (1999) 3979.
[18] C.H. Yang, H.J. Yang, T.C. Wen, M.S. Wu, J.S. Chang, Polymer 40 (1999) 871.
[19] T.C. Wen, J.S. Chang, T.T. Cheng, J. Electrochem. Soc. 145 (1998) 3450.
[20] T.T. Cheng, T.C. Wen, J. Electroanal. Chem. 459 (1998) 99.
[21] T.T. Cheng, T.C. Wen, Solid State Ionics 107 (1998) 161.
[22] C.H. Yang, Y.J. Li, T.C. Wen, Ind. Eng. Chem. Res. 36 (1997) 1614.
[23] T.C. Wen, Y.J. Wang, Ind. Eng. Chem. Res. 38 (1999) 1415.
[24] T.C. Wen, W.C. Chen, J. Appl. Polym. Sci., accepted for publication, 1999.
[25] R. Huq, R. Koksbang, P.E. Toner, G.C. Farrington, Electrochim. Acta 37 (1992) 1681.
[26] F. Croce, F. Gerace, G. Dautzemberg, S. Passerini, G.B. Appetecchi, B. Scrosati, Electrochim. Acta 39 (1994) 2187.
[27] J.M. Tarascon, D. Guyomard, Solid State Ionics 69 (1994) 293.
[28] J.N. Reimers, J.R. Dahn, J. Electrochem. Soc. 139 (1992) 2091.
[29] J. Kleinberg, W.J. Argersinger, E. Griswold, Inorganic Chemistry, D.C Heath and Company, Boston, 1960, pp. 550–551.